Small Molecules

DOI: 10.1002/anie.201302968

The Iminyl Radical O_2SN**

Xiaoqing Zeng, Helmut Beckers,* and Helge Willner*

Dedicated to Prof. Werner Uhl on the occasion of his 60th birthday

Sulfonylazides, RSO_2N_3, are widely used diazo[1] and azide[2] transfer reagents, and in particular the photolytic or thermal elimination of N_2 from these azides have been well-studied.[3] Although the latter routes are generally used for the in situ generation of sulfonyl nitrenes, RSO_2N, both were found to be complicated owing to secondary product formation, such as $SO_2 + RN$, as well as the pseudo Curtius rearrangement product $RN{=}SO_2$.[3,4]

Recently it became apparent that initially formed reactive singlet sulfonyl nitrenes might be rapidly quenched by efficient intersystem crossing (ISC) to yield the lower-energy triplet nitrenes of sluggish reactivity.[4] Thermally persistent triplet FSO_2N was produced by flash pyrolysis (ca. 800 °C) of FSO_2N_3 in yields up to 66 %.[5] Only traces of SO_2 and FSO_2 were found as byproducts, and the lifetime of triplet FSO_2N in the gas phase was found to be dominated by precursor concentration-dependent triplet nitrene dimerization.[5] Triplet nitrenes, produced by flash-pyrolysis of selected azides, have also offered unique access to synthetically challenging molecules, such as OCN–NCO,[6] *cyclo*-N_2CO,[7] OPN/ONP,[8] SPN/SNP/*cyclo*-PSN,[9] and the FSO_2 radical.[5]

Herein, we extend our flash vacuum pyrolysis studies to the simple alkyl sulfonyl azides $CF_3SO_2N_3$ and $CH_3SO_2N_3$, and present the detection and the photochemistry of the novel O_2SN (sulfonyliminyl) radical.

Flash vacuum pyrolysis of $CF_3SO_2N_3$ highly diluted in argon (1:500) was performed by passing the gas mixture through a hot quartz furnace (ca. 800 °C, inside diameter 1.0 mm, length 30 mm). The reaction mixture was immediately deposited onto the cold matrix support (16 K) in a high vacuum (see the Supporting Information for details). The IR spectrum of the deposit reveals almost complete decomposition of the azide (Supporting Information, Figure S1). Along with the known IR bands of SO_2, SO_3, CF_3, and C_2F_6, there are a number of new IR bands showing distinct ^{15}N isotopic shifts in experiments using a mixture of $CF_3SO_2{}^{15}N_\alpha NN$ and $CF_3SO_2NN^{15}N_\gamma$ (1:1). To distinguish between different possible carriers of the new IR bands, the deposit was subjected to light with wavelength $\lambda > 360$ nm and radiation from a 365 nm LED source, which both were found to efficiently deplete the same set of the new bands. The mid-IR difference spectrum obtained from the first experiment is shown in Figure 1.

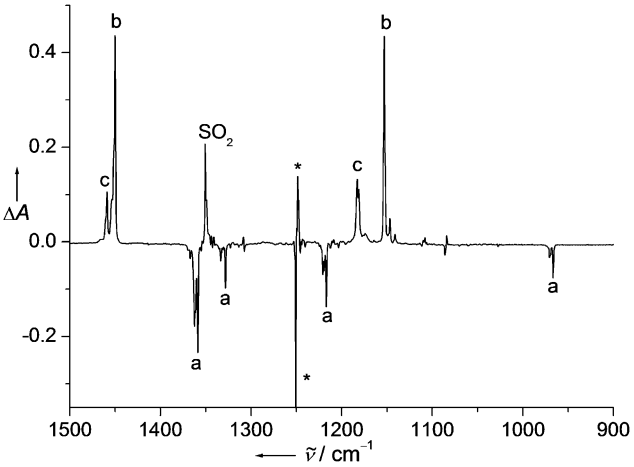

Figure 1. IR spectral changes in the region of 1500–900 cm^{-1} obtained after photolysis ($\lambda > 360$ nm) of Ar matrix-isolated (16 K) pyrolysis products of $CF_3SO_2N_3$. Bands assigned to O_2SN (a) decreased, and bands that are due to SO_2, *syn* (b) and *anti* OSNO (c) appeared. Residual bands of the CF_3 radical (marked by asterisks) occurred in the difference spectrum owing to matrix site changes upon photolysis.

Based on their same photolytic behavior, four IR bands at 1358.6, 1328.3, 1216.9, and 966.9 cm^{-1} in the mid-IR spectrum (Figure 1, a) are assigned to species a. Its IR spectrum was completed by recording three additional bands in the far-IR region (Figure 2) at 474.5, 413.2, and 367.6 cm^{-1}. Each band exhibits a satellite that is due to matrix sites, and along with the complete set of $^{14/15}N$ isotopic shifts, bands associated with the naturally abundant ^{34}S isotopologue were also observed. The experimental vibrational data are compared in Table 1 with predicted values for the planar O_2SN (C_{2v}) radical obtained at the DFT B3LYP/6-311 + G(3df) level. With the exception of the band at 1328.3 cm^{-1}, the agreement is very good. This band is attributed to the combination 966.9 (a_1) + 367.6 (b_2) = 1334.5 cm^{-1} (b_2), which takes intensity through a Fermi resonance from the strong fundamental at 1358.6 cm^{-1} (b_2). Apart from the six fundamentals, two combination and two overtone bands of O_2SN were observed and assigned.

The assignment of the IR spectrum of O_2SN is given in Table 1. The two strongest bands at 1358.6 and 1216.9 cm^{-1} are readily attributed to antisymmetric (ν_5) and symmetric

[*] Prof. Dr. X.-Q. Zeng
College of Chemistry, Chemical Engineering and Materials Science
Soochow University, 215123 Suzhou (China)
E-mail: xqzeng@suda.edu.cn
Dr. H. Beckers, Prof. Dr. H. Willner
FB C-Anorganische Chemie, Bergische Universität Wuppertal
Gaussstrasse 20, 42119 Wuppertal (Germany)
E-mail: beckers@uni-wuppertal.de

[**] Support from the Deutsche Forschungsgemeinschaft (DFG) (WI 663/26-1) for this work, and in particular for funding a research stay of X.-Q.Z. in Wuppertal, is gratefully acknowledged.

Supporting information for this article is available on the WWW under http://dx.doi.org/10.1002/anie.201302968.

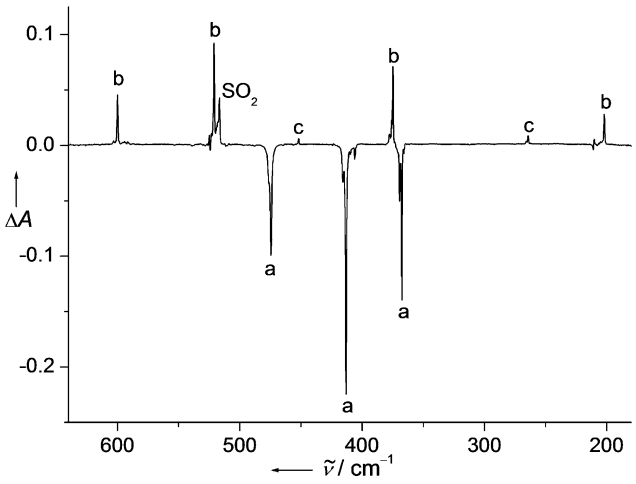

Figure 2. IR spectral changes in the far-IR region of 640–180 cm^{-1} obtained after irradiation ($\lambda > 360$ nm) of the Ar matrix-isolated (16 K) pyrolysis products of $CF_3SO_2N_3$. Bands assigned to O_2SN (a) decreased, and bands due to SO_2, *syn* (b) and *anti* OSNO (c) appeared.

Table 1: Observed and calculated IR frequencies ν, isotope shifts $\Delta\nu$ (cm^{-1}) and band assignments for the O_2SN ($^2B_2$, C_{2v}) radical.

ν		$\Delta\nu$ ($^{14/15}$N)		$\Delta\nu$ ($^{32/34}$S)		Mode
expt (Ar)[a]	calcd[b]	expt	calcd	expt	calcd	ν_i[c]
2700.8 (1)		< 0.5				$2\nu_5$
2561.0 (1)		8.6				$\nu_1+\nu_5$
2424.5 (2)		13.0				$2\nu_1$
1358.6 (100)	1336 (156)	1.7	0.1	16.5	17.4	ν_5, $\nu_{as}(SO_2)$
1328.3 (18)		21.9				$\nu_3+\nu_6$
1216.9 (37)	1201 (46)	6.5	6.4	13.5	14.0	ν_1, $\nu_s(SO_2)$
966.9 (15)	954 (9)	17.8	19.2	1.2	1.1	ν_2, ν(SN)
474.5 (26)	462 (19)	1.4	1.5	2.4	2.5	ν_3, $\delta(SO_2)$
413.2 (38)	414 (20)	1.8	1.9	7.1	7.5	ν_4, $\delta_{o.o.p.}$
367.6 (22)	358 (20)	6.0	6.0	1.8	1.8	ν_6, δ(OSN)

[a] Band positions of the most intense matrix sites in solid argon at 16 K, and relative intensities (in parenthesis) based on integrated areas of all matrix sites. [b] Harmonic frequencies calculated at the DFT B3LYP/6-311+G(3df) level of theory and scaled by a factor of 0.9679. Calculated IR intensities (km mol^{-1}) are given in parentheses. [c] Numbering of fundamentals ν_i (i=1–6) according to their symmetry (a_1: i=1–3, b_1: 4, b_2: 5 and 6) and frequency.

(ν_1) stretches of a SO_2 moiety, respectively, and the assignment of the SN stretch (ν_2) to the band at 966.9 cm^{-1} is supported by its large ^{15}N isotope shift of 17.8 cm^{-1}. A significant ^{34}S isotope shift for the band at 413.2 cm^{-1} is consistent with its assignment to an out-of-plane mode ν_4 of the planar radical. Thus, the band at 474.5 cm^{-1} should be attributed to the SO_2 bending mode (ν_3), which is lower in frequency than that of free SO_2 (516.7 cm^{-1}, Ar matrix) owing to vibrational coupling with the SN stretch in O_2SN, and the lowest energy vibration at 367.6 cm^{-1} to the OSN bending mode ν_6. We note that the O_2SN radical was also detected among the flash pyrolysis products of $CH_3SO_2N_3$ (Supporting Information, Figure S2). However, the main products were SO_2 and CH_2NH, and the yield of O_2SN was significantly lower compared to that found by pyrolysis of $CF_3SO_2N_3$.

The identification of the photolysis products of O_2SN is straightforward. Traces of SO_2 formed during UV irradiation ($\lambda > 360$ nm) of Ar matrix-isolated O_2SN (Figure 1) indicate its photodecomposition into SO_2 and nitrogen atoms. Apart from the known SO_2 bands, strong bands appeared at 1450.3 and 1152.9 cm^{-1} (Figure 1, b) and weaker bands at 1459.2 and 1182.9 cm^{-1} (Figure 1, c). These band positions are close to reported NO and SO stretching frequencies for the open-chain molecules *syn* OSNO (1450.8 and 1154.9 cm^{-1}) and *anti* OSNO (1456.0 and 1181.2 cm^{-1}) isolated in argon matrices.[10] Large ^{15}N isotope shifts obtained for the NO stretches (*syn* 24.9 cm^{-1}, *anti* 24.8 cm^{-1}) support their assignment, whereas the SO stretches are much less affected by ^{15}N isotopic substitution (Supporting Information, Figure S3).

In previous work, the bent OSNO isomers were obtained in low yield by laser photolysis (248 nm) of matrices containing OCS and NO_2.[10] Only their two strongest IR bands were observed, and the presence of a CO molecules along with the OSNO radicals in the matrix cage are responsible for the differences between reported and our band positions. IR radiation from the globar source was found to convert *anti* OSNO to the more stable *syn* isomer.[10] We also observed this conversion using 365 nm LED radiation.

The efficient photoisomerization of O_2SN (C_{2v}) into the chain-like OSNO (C_S) radicals allows for a more complete analysis of their IR spectra (Figure 2). Their vibrational data are summarized in Table 2 and Table 3, respectively. For the *syn* isomer the weak SN stretching band (ν_3) appeared at

Table 2: Observed and calculated IR frequencies ν and isotope shifts $\Delta\nu$ (cm^{-1}) for *syn* OSNO ($^2A'$, C_S).

ν		$\Delta\nu$ ($^{14/15}$N)		$\Delta\nu$ ($^{32/34}$S)		Mode
expt (Ar)[a]	calcd[b]	expt	calcd	expt	calcd	
2866.7 (6)		48.3		< 0.5		$2\nu_1$
1450.3 (100)	1461 (188)	24.9	25.9	< 0.5	0.2	ν_1, ν(NO)
1152.9 (87)	1144 (183)	2.3	0.3	11.8	11.8	ν_2, ν(SO)
600.2 (4)	614 (3)	5.6	7.0	8.4	8.9	ν_3, ν(SN)
521.2 (15)	520 (18)	10.9	11.2	2.3	2.6	ν_4, δ(OSN)
375.0 (11)	393 (9)	7.5	8.1	1.8	2.0	ν_5, δ(ONS)
202.2 (4)	200 (3)	< 0.5	0.4	< 0.5	0.3	ν_6, τ

[a] Band position of the most intense matrix site in solid argon at 16 K, relative intensities (in parenthesis) based on the integrated areas of all matrix sites. [b] Harmonic frequencies calculated at the B3LYP/6-311+G(3df) level of theory and scaled by a factor of 0.9679; calculated IR intensities [km mol^{-1}] are given in parentheses.

600.2 cm^{-1} (Figure 2, b) along with three additional deformations in the far-IR region. Owing to a lower abundance of the less-stable *anti* conformer, the assignment of its weak SN stretch is difficult. A weak overtone band $2\nu_1$ was however observed for both isomers.

Upon 266 nm laser irradiation, *syn* OSNO rearranged into the less stable *anti* isomer. Using mercury arc radiation ($\lambda >$ 255 nm), traces of SNO radicals were also detected by means of two weak IR bands at 1593.3 ($2\nu_2$, $\Delta\nu$ ($^{14/15}$N) = 28.3 cm^{-1}) and 1522.6 cm^{-1} (ν_1, $\Delta\nu$ ($^{14/15}$N) = 24.7 cm^{-1})[11] (Supporting Information, Figure S4).

Table 3: Observed and calculated IR frequencies ν and isotope shifts $\Delta\nu$ (cm^{-1}) for *anti* OSNO ($^2A'$, C_S).

ν expt (Ar)[a]	calcd[b]	$\Delta\nu$ ($^{14/15}N$) expt	calcd	Mode
2887.3 (2)		49.8		$2\nu_1$
1459.2 (67)	1471 (253)	24.8	26.7	ν_1, ν(NO)
1182.9 (100)	1162 (206)	1.0	0.1	ν_2, ν(SO)
	582 (2)		10.9	ν_3, ν(SN)
452.0 (2)	451 (5)	3.8	4.0	ν_4, δ(OSN)
272.6 (<1)	279 (0.3)	4.7	5.3	ν_6, τ
264.4 (3)	261 (8)	2.1	2.1	ν_5, δ(ONS)

[a] Band position of the most intense matrix site in solid argon at 16 K, relative intensities (in parenthesis) based on the integrated areas of all matrix sites. [b] Harmonic frequencies calculated at the B3LYP/6-311+G(3df) level of theory and scaled by a factor of 0.9679; the calculated IR intensities [km mol^{-1}] are given in parentheses.

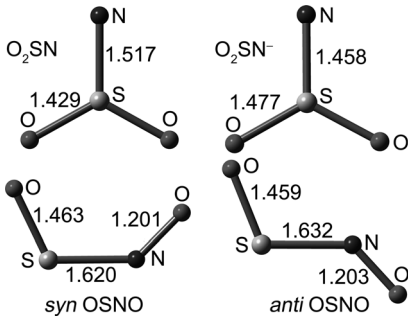

Figure 3. Calculated planar molecular structures (bond lengths in Å) of O_2SN ($^2B_2$, ∠OSO = 121.7°), O_2SN^- ($^1A_1$, ∠OSO = 110.1°), *syn* OSNO ($^2A'$, ∠OSN = 115.3°, ∠SNO = 134.9°), and *anti* OSNO ($^2A'$, ∠OSN = 111.9°, ∠SNO = 132.5°) at the B3LYP/6-311+G(3df) level of theory.

In the initially obtained IR spectrum of the pyrolysis products of $CF_3SO_2N_3$, some bands remained unassigned. They also revealed distinct ^{15}N isotope shifts (Supporting Information, Figure S5), but remained almost unaffected by any of the aforementioned irradiations. These bands appeared at 1413.1, 1313.6, 1243.8, 1213.1, 1196.3, and 1045.4 cm^{-1}, indicating the presence of SO_2 (1413.1, 1045.4 cm^{-1}) and CF_3 (1243.8, 1213.1, 1196.3 cm^{-1}) group vibrations. A large ^{15}N isotope shifts (19.3 cm^{-1}) for the strong band at 1313.6 cm^{-1} suggests an S=N stretching band. IR frequencies calculated for the most likely carrier, *N*-sulfonyl imine $CF_3N{=}SO_2$, fit very well with the observations (Supporting Information, Table S1). Three weaker far-IR bands at 585.3, 471.9, and 406.0 cm^{-1} were also assigned to this species.

The identification of intermediates from the flash pyrolysis of sulfonyl azides RSO_2N_3 (R = CH_3, CF_3) sheds light on their thermal decomposition mechanism and the formation of O_2SN. Upon pyrolysis, both azides are expected to eliminate N_2 furnishing the short-lived singlet nitrene RSO_2N. Initially formed singlet RSO_2N may undergo: 1) ISC to the triplet ground state; 2) Curtius-type rearrangement to $RN{=}SO_2$; or 3) R–S bond fission to yield the radical pair O_2SN and R. The favorable formation of O_2SN by flash pyrolysis of $CF_3SO_2N_3$ according to (3) is consistent with the weak $F_3C^{\delta+}$-$S^{\delta+}$ bond in the nitrene, CF_3SO_2N, for which a dissociation energy of 66 kJ mol^{-1} (singlet CF_3SO_2N) is predicted by preliminary calculations using the complete basis set CBS-QB3 method.[12] For the methyl analogue, the C–S bond energies of singlet CH_3SO_2N is considerably higher (117 kJ mol^{-1}), suggesting (2) and (3) are competing processes in the flash pyrolysis of $CH_3SO_2N_3$. The Curtius-type rearrangement (2) eventually yields fragments (SO_2 and CH_2NH) of CH_3NSO_2, although their formation by radical reactions between CH_3 and NSO_2, formed under the pyrolysis conditions, cannot be excluded.

In recent studies on NO_2S species,[10,13] the planar O_2SN radical was not considered at all. We have calculated the molecular structures and energies of various planar NO_2S isomers on the doublet potential energy surface using different theoretical methods (Supporting Information, Table S2). At all of the levels applied, *syn* OSNO ($^2A'$, Figure 3) was found to be the lowest-energy isomer, O_2SN ($^2B_2$) and *anti* OSNO ($^2A'$, Figure 3) were found to be slightly higher in energy by, respectively, 17.4 (13.6) kJ mol^{-1} and 15.2 (17.3) kJ mol^{-1} at the CCSD(T)//MP2 (CBS-QB3) levels of theory. We note the existence of another weakly interacting *syn* OS···NO minimum (SN 2.047 Å; Supporting Information, Table S2), having the unpaired electron in a bonding a″ orbital; however, in the following we will focus on the experimentally confirmed isomers only.

DFT calculations predict a planar molecular structure of C_{2v} symmetry for the O_2SN radical (Figure 3). A comparison with the related structure of the *N*-sulfonyl imine $CF_3N{=}SO_2$, calculated at the same level of theory (see Supporting Information), revealed similar S=O bond lengths and OSO angles (O_2SN: 1.429 Å (S=O), ∠OSO = 121.7°; $CF_3N{=}SO_2$: 1.427 and 1.422 Å (S=O), ∠OSO = 121.7°) for these two related molecules. The S=N bond in O_2SN (1.517 Å) is slightly longer than that of CF_3NSO_2 (1.507 Å).

Although O_2SN ($^2B_2$) is isostructural and isoelectronic to the known FCO_2 ($^2B_2$) radical,[14] the electronic structures of these two radicals are very different. The electron spin density of FCO_2 is equally shared between the two oxygen atoms,[14] but localized at the nitrogen atom in O_2SN. Calculations for the closed-shell O_2SN^- anion (Figure 3)[15] reveal a significantly shortened S=N (1.458 Å) associated with elongated S=O bond lengths (1.477 Å), indicating that the unpaired electron in O_2SN resides in a π(NS) bonding (b_2) molecular orbital. The O_2SN^- anion is isoelectronic to recently detected F_2PN.[16] According to natural bond orbital (NBO) analysis, two doubly occupied atomic p-type orbitals of nitrogen in these molecules are engaged in π bonding to the central atom, whereas in the O_2SN radical the corresponding in-plane (b_2) HOMO is only half-filled (Supporting Information, Figure S6, Table S3). The lowest-energy transition between the highest doubly occupied b_1 and the singly occupied b_2 orbitals in O_2SN is forbidden by symmetry (A_2). However, time-dependent (TD) DFT calculations predict reasonably strong UV bands at 322 (A_1, $f = 0.0094$), 224 (B_1, 0.0025) and 217 nm (B_2, 0.0074). These predictions are consistent with the observed photosensitivity of O_2SN and the presence of two structured UV absorptions centered at $\lambda_{max} \approx 350$ nm and below 250 nm (Supporting Information, Figure S7). The latter absorption shows a regular vibrational spacing of about 490 cm^{-1}. These absorptions are associated with O_2SN, as they

vanished completely after irradiation with light of $\lambda > 360$ nm (Supporting Information, Figures S8 and S9).

The SN bond lengths predicted for the planar bent OSNO isomers of 1.62–1.63 Å (Figure 3) are between the expected values for single (1.74 Å) and double SN bonds (1.54 Å).[17] In a MO scheme, bonding interactions between the diatomic fragments OS and NO may arise from a combinations of their partially filled π* fragment orbitals (for the frontier molecular orbitals, see the Supporting Information, Figure S6). For the bent $OSNO^-$ anion (24 valence electrons), the corresponding in-plane (a′) and out-of-plane (a″) (π*π*) bonding interactions affords a formal S=N double bond (Supporting Information, Table S4). For OSNO (23 valence electrons), the unpaired electron resides in the a′ bonding combination (Supporting Information, Figure S6). However, the spin densities for *syn* and *anti* OSNO were calculated to be localized mainly at the NO moiety.

A strong UV absorption at $\lambda_{max} \approx 285$ nm with a regular vibrational spacing of about 1000 cm^{-1} occurred in the experimental spectrum after UV photolysis of O_2SN (Supporting Information, Figure S7), which is most likely associated with the bent OSNO ($^2A'$) radicals. This assignment is supported by TD DFT calculations, which predict strong UV transitions ($f > 0.09$) for *syn* and *anti* OSNO at 266 and 269 nm, respectively (Supporting Information, Figure S7). The *anti* to *syn* interconversion was predicted to proceed by a low-energy N-inversion process rather than by S–N bond rotation, and for both isomers low barriers of less than 40 kJ mol^{-1} were reported for their dissociation into the diatomic fragments OS + NO.[13] In contrast, the thermally robust nature of the O_2SN radical is confirmed by the absence of SO and NO in the flash pyrolysis products. On the other hand, photoisomerization from O_2SN to bent OSNO radicals may proceed either via a cyclic transition state or by photodissociation and recombination of the photofragments OSN + O in a matrix cage. The dissociative mechanism has been suggested for the rearrangement of the related molecules NO_3 ($\rightarrow ON + O_2$)[18] and SO_3 ($\rightarrow OSOO$).[19]

In summary, flash vacuum pyrolysis of sulfonyl azides, $CF_3SO_2N_3$ and $CH_3SO_2N_3$, yields the planar O_2SN ($^2B_2$) radical. IR and UV spectra of the novel radical have been assigned and its photorearrangement into the planar bent isomers, *syn* and *anti* OSNO ($^2A'$), has been observed in solid noble-gas matrices. The facile generation of O_2SN in the gas phase from two easily accessible azides will stimulate further studies on its spectroscopy, structure, and chemistry.

Received: April 10, 2013
Published online: June 20, 2013

Keywords: azides · flash pyrolysis · IR spectroscopy · nitrenes · rearrangement

[1] J. Raushel, S. M. Pitram, V. V. Fokin, *Org. Lett.* **2008**, *10*, 3385–3388, and references therein.
[2] P. Panchaud, L. Chadaud, Y. Landais, C. Ollivier, P. Renaud, S. Zigmantas, *Chem. Eur. J.* **2004**, *10*, 3606–3614, and references therein.
[3] For examples, see: a) W. Lwowski, E. Scheiffele, *J. Am. Chem. Soc.* **1965**, *87*, 4359–4365; b) R. A. Abramovitch, C. I. Azogu, I. T. McMaster, *J. Am. Chem. Soc.* **1969**, *91*, 1219–1220; c) R. A. Abramovitch, G. N. Knaus, V. Uma, *J. Am. Chem. Soc.* **1969**, *91*, 7532–7533; d) D. S. Breslow, E. I. Edwards, E. C. Linsay, H. Omura, *J. Am. Chem. Soc.* **1976**, *98*, 4268–4275; e) J.-C. Garay, V. Maloney, M. Marlow, P. Small, *J. Phys. Chem.* **1996**, *100*, 5788–5793.
[4] a) S. Vyas, J. Kubicki, H. L. Luk, Y. Zhang, N. P. Gritsan, C. M. Hadad, M. S. Platz, *J. Phys. Org. Chem.* **2012**, *25*, 693–703; b) J. Kubicki, Y. Zhang, S. Vyas, G. Burdzinski, H. L. Luk, J. Wang, J. Xue, H. L. Peng, E. A. Pritchina, M. Sliwa, G. Buntinx, N. P. Gritsan, C. M. Hadad, M. S. Platz, *J. Am. Chem. Soc.* **2011**, *133*, 9751–9761, and references therein.
[5] X. Q. Zeng, H. Beckers, H. Willner, *J. Am. Chem. Soc.* **2013**, *135*, 2096–2099.
[6] G. Maier, M. Naumann, H. P. Reisenauer, J. Eckwert, *Angew. Chem.* **1996**, *108*, 1800–1801; *Angew. Chem. Int. Ed. Engl.* **1996**, *35*, 1696–1697.
[7] a) X. Q. Zeng, H. Beckers, H. Willner, J. F. Stanton, *Angew. Chem.* **2011**, *123*, 1758–1761; *Angew. Chem. Int. Ed.* **2011**, *50*, 1720–1723; b) X. Q. Zeng, H. Beckers, H. Willner, J. F. Stanton, *Eur. J. Inorg. Chem.* **2012**, 3403–3409.
[8] X. Q. Zeng, H. Beckers, H. Willner, *J. Am. Chem. Soc.* **2011**, *133*, 20696–20699.
[9] X. Q. Zeng, H. Beckers, H. Willner, J. S. Francisco, *Angew. Chem.* **2012**, *124*, 3390–3395; *Angew. Chem. Int. Ed.* **2012**, *51*, 3334–3339.
[10] M. Bahou, Y. P. Lee, *J. Chem. Phys.* **2001**, *115*, 10694–10700.
[11] M. Hawkins, A. J. Downs, *J. Phys. Chem.* **1984**, *88*, 3042–3047.
[12] J. A. Montgomery, M. J. Frisch, J. W. Ochterski, G. A. Petersson, *J. Chem. Phys.* **1999**, *110*, 2822–2827.
[13] W.-C. Chen, C.-H. Yu, *J. Chem. Phys.* **2001**, *115*, 7495–7502.
[14] H. Beckers, H. Willner, D. Grote, W. Sander, J. Geier, *J. Chem. Phys.* **2008**, *128*, 224301–224307.
[15] a) H. W. Roesky, W. Schmieder, W. Isenberg, D. Böhler, G. M. Sheldrick, *Angew. Chem.* **1982**, *94*, 143; *Angew. Chem. Int. Ed. Engl.* **1982**, *21*, 153; b) N. H. Morgon, H. V. Linnert, J. M. Riveros, *J. Phys. Chem.* **1995**, *99*, 11667–11672; c) R. Mews, P. G. Watson, E. Lork, *Coord. Chem. Rev.* **1997**, *158*, 233–273.
[16] X. Q. Zeng, H. Beckers, H. Willner, *Angew. Chem.* **2009**, *121*, 4922–4925; *Angew. Chem. Int. Ed.* **2009**, *48*, 4828–4831.
[17] P. Pyykkö, M. Atsumi, *Chem. Eur. J.* **2009**, *15*, 12770–12779.
[18] M. P. Grubb, M. L. Warter, H. Xiao, S. Maeda, K. Morokuma, S. W. North, *Science* **2012**, *335*, 1075–1078.
[19] S. H. Jou, M. Y. Shen, C. H. Yu, Y. P. Lee, *J. Chem. Phys.* **1996**, *104*, 5745–5753.

